Journal of Geoscience and Environment Protection, 2026, 14(6), 74-97
https://www.scirp.org/journal/gep
ISSN Online: 2327-4344
ISSN Print: 2327-4336

Spatial and Statistical Analysis of Groundwater Chemical Composition in Mui Basin Block C, Kitui County, Kenya: Relationships among pH, Nitrates, and Total Dissolved Solids

Nurh Kipkorir Kibos[1*], Julian A. Ogondo[2], Noah Kerandi[1]

[1]Department of Geology and Meteorology, School of Agriculture, Environment, Water and Natural Resources, South Eastern Kenya University, Kitui, Kenya
[2]Department of Geography and Natural Resource Management, School of Arts and Social Sciences, Maseno University, Kisumu, Kenya
Email: *kibosnurh@gmail.com

How to cite this paper: Kibos, N. K., Ogondo, J. A., & Kerandi, N. (2026). Spatial and Statistical Analysis of Groundwater Chemical Composition in Mui Basin Block C, Kitui County, Kenya: Relationships among pH, Nitrates, and Total Dissolved Solids. *Journal of Geoscience and Environment Protection, 14,* 74-97.
https://doi.org/10.4236/gep.2026.146005

Received: April 28, 2026
Accepted: June 19, 2026
Published: June 22, 2026

Copyright © 2026 by author(s) and Scientific Research Publishing Inc.
This work is licensed under the Creative Commons Attribution International License (CC BY 4.0).
http://creativecommons.org/licenses/by/4.0/
Open Access

Abstract

Groundwater quality assessment is critical for sustainable water resource management in arid and semi-arid regions. This study investigated the spatial distribution and interrelationships among pH, nitrate concentrations, and total dissolved solids (TDS) in groundwater from Mui Basin Block C, Mwingi Central, Kitui County, Kenya. Water samples were collected from all existing 32 sampling points comprising boreholes, shallow wells, and earth dams, representing shallow (1 - 10 m), moderate (10 - 30 m), and deep (>30 m) aquifer systems. Physicochemical analysis was conducted following standard methods, and spatial distribution patterns were mapped using Inverse Distance Weighting (IDW) interpolation in ArcGIS. Statistical analyses, including descriptive statistics, one-way ANOVA, and Pearson correlation, were performed to examine relationships among parameters. Results revealed mean values of pH 7.84 ± 0.89, TDS 964.74 ± 893.76 mg/L, and nitrate 56.11 ± 44.52 mg/L. ANOVA indicated no significant variation in these parameters across different aquifer depths ($p > 0.05$), suggesting uniform hydrogeochemical processes throughout the basin. Strong positive correlations were observed between electrical conductivity and TDS ($r = 0.99$, $p < 0.01$), and moderate correlations between nitrate and salinity parameters. Spatial analysis revealed elevated TDS and nitrate concentrations in the central and southeastern portions of the basin, likely influenced by geological formations, agricultural activities, and limited recharge. The findings indicate that groundwater quality in Mui Basin

Block C is primarily controlled by water-rock interactions and anthropogenic inputs rather than aquifer depth, with implications for targeted water quality management strategies in similar semi-arid environments.

Keywords

Groundwater Quality, PH, Nitrates, Total Dissolved Solids, Spatial Analysis, IDW Interpolation, Mui Basin

1. Introduction

Groundwater resources constitute a vital water supply source for communities in arid and semi-arid lands (ASALs) of Kenya, where surface water availability is limited and highly seasonal (Derdour et al., 2020). Kitui County, located in the Eastern region of Kenya, experiences chronic water scarcity due to low and erratic rainfall patterns, high evapotranspiration rates, and limited surface water storage infrastructure (Hassan et al., 2023). The Mui Basin in Block C of Mwingi Central sub-county represents a critical groundwater resource zone serving domestic, agricultural, and livestock water needs for local communities [(Government of Kenya, 2018) "Kitui County Integrated Development Plan, 2018-2022]. In semi-arid regions of East Africa, groundwater quality is increasingly threatened by both natural hydrogeochemical processes and anthropogenic activities, necessitating comprehensive assessment frameworks that integrate spatial and statistical approaches (Sodomon et al., 2025; Pradhan et al., 2023).

Understanding the chemical composition of groundwater and the spatial relationships among key water quality parameters is essential for sustainable groundwater management and protection (Ashun & Tagoe, 2024). Among the critical parameters, pH influences the solubility and mobility of chemical constituents (Drias et al., 2023). Total dissolved solids (TDS) indicate overall water mineralisation and suitability for various uses (Nicholas, 2023; Al Mousawi et al., 2023), and nitrate concentrations reflect both natural processes and anthropogenic contamination, particularly from agricultural activities and sanitation systems (Bulle, 2025; Hagage et al., 2022). In basement aquifer systems characteristic of the Mozambique Belt crystalline rocks in Kenya, hydrogeochemical evolution is primarily controlled by silicate weathering, water-rock interactions, and residence time (Abdessamed et al., 2023; Loh et al., 2020). These processes result in distinctive spatial patterns of groundwater quality that require geostatistical analysis for proper characterization (Gomaa et al., 2023).

Previous hydrogeochemical studies in semi-arid regions of Kenya and East Africa have documented significant spatial variability in groundwater quality, influenced by factors including geological formations, residence time, recharge patterns, and human activities (Ashun & Tagoe, 2024; Obrike et al., 2023). Recent investigations in the Upper Athi River Basin of Kenya have demonstrated that

anthropogenic drivers, particularly agricultural practices and inadequate sanitation infrastructure, significantly impair groundwater quality in shallow aquifer systems (Ashun & Tagoe, 2024). Similarly, studies in basement aquifers across West Africa have shown that crystalline rock weathering and anthropogenic inputs jointly control groundwater chemistry, with nitrate contamination emerging as a primary concern in agricultural areas (Sodomon et al., 2025; Loh et al., 2020; Adagba et al., 2022). However, comprehensive spatial and statistical analyses correlating pH, nitrates, and TDS in the Mui Basin remain limited (Water Resources Authority, 2013; Tanathi Water Works Development Agency, 2019). Such analyses are crucial for identifying contamination hotspots, understanding hydrogeochemical processes, and developing targeted water quality management interventions and plans (Sunitha & Reddy, 2022; Radelyuk et al., 2020).

Geographic Information Systems (GIS) coupled with geostatistical interpolation methods, particularly Inverse Distance Weighting (IDW) and kriging, have proven effective for mapping groundwater quality parameters and identifying spatial trends in semi-arid areas (Hassan et al., 2023; Bind & Kanchan, 2020; Mohallel, 2024; Saraswat et al., 2023). These spatial analysis techniques enable visualisation of contamination patterns and support evidence-based decision-making for water resource management (Ekwule et al., 2023; Javed et al., 2024). The integration of spatial analysis with multivariate statistical methods provides a robust framework for understanding the complex relationships among water quality parameters and their controlling factors (Mythilee Priyanka et al., 2023; Muniz et al., 2023).

The primary objective of this study was to relate the chemical composition of groundwater pH, nitrates, and total dissolved solids in Mui Basin Block C through integrated spatial and statistical approaches. Specific aims included: 1) characterising the spatial distribution patterns of pH, TDS, and nitrate using geostatistical interpolation methods; 2) examining variations in these parameters across different aquifer depths; and 3) determining the statistical relationships and correlations among the parameters to elucidate controlling hydrogeochemical processes.

This research contributes to the growing body of knowledge on groundwater quality in Kenya's ASALs and provides evidence-based information to support water resource planning, quality monitoring programs, and community water supply interventions in the Mui Basin and similar hydrogeological settings.

2. Methodology

2.1. Study Area

The study was conducted in Mui Basin Block C, located in Mwingi Central subcounty, Kitui County, in the Eastern region of Kenya. The basin lies within the semi-arid climatic zone characterised by bimodal rainfall patterns with long rains (March-May) and short rains (October-December), averaging 500 - 800 mm annually. The area experiences high temperatures ranging from 18˚C to 34˚C and high potential evapotranspiration rates exceeding 2000 mm per year, resulting in

significant moisture deficits.

Geologically, the Mui Basin is underlain by Precambrian basement rocks of the Mozambique Belt, comprising predominantly metamorphic rocks including gneisses, schists, and migmatites, with intrusions of granitic rocks. Quaternary sediments, including alluvial deposits, colluvium, and weathered materials in valley bottoms and drainage channels, overlie these crystalline basement rocks. The hydrogeological system comprises weathered and fractured aquifer zones within the basement complex, with groundwater occurrence controlled by the degree of weathering, fracture density, and fracture connectivity.

The study area covers approximately 450 km^2 and is drained by seasonal rivers and streams that flow during the rainy seasons. Land use in the basin is predominantly smallholder agriculture (maize, beans, sorghum, and millet), livestock grazing, and scattered settlements. Groundwater is accessed through boreholes, shallow hand-dug wells, and earth dams, serving as the primary water source for the population estimated at over 50,000 people.

2.2. Sample Collection and Analysis

The 32 sampling points used in this study represent the complete inventory of accessible water points in Mui Basin Block C at the time of fieldwork, as enumerated from the Tanathi Water Works Development Agency (TaWWDA) water-point registry; no additional points were excluded. The sampling points comprised 23 boreholes (BH), 7 shallow wells (SW), and 2 earth dams (ED), with borehole and well depths ranging from 15.7 m to 262.7 m. The two earth dams were retained in the dataset because they interact with the shallow groundwater system through bank infiltration and seepage, and their chemical signatures are informative for characterising surface-groundwater exchange in the basin; however, their data were analysed separately where appropriate to avoid conflation with strictly subsurface sources. Based on total well depth, sampling points were categorised into three groups: shallow (1 - 10 m, n = 10), moderate (10 - 30 m, n = 11), and deep (>30 m, n = 11) aquifer systems.

Geographical coordinates of each sampling point were recorded using a handheld GPS device (Garmin eTrex 30x) with an accuracy of ±3 m. All 32 sampling points were visited and sampled once during a single field campaign conducted between August and November 2025, corresponding to the late dry season transitioning into the short-rains (October-December) hydrological season. Because each site was sampled only once, the reported concentrations represent a snapshot of conditions during that period; seasonal variation in nitrate and salinity, which can be pronounced in semi-arid settings due to dilution during recharge events and concentration during dry periods, could not be assessed from this dataset. Water samples were collected following standard protocols for groundwater sampling. At each borehole, water was pumped for 10 - 15 minutes to purge stagnant water from the well casing before sample collection. For shallow wells, samples were collected using clean bailers to avoid surface contamination. All samples were col-

lected in pre-cleaned 1-liter polyethylene bottles that had been rinsed three times with the sample water before final collection.

Physicochemical parameters were analysed at the Water Resources Authority (WARMA) laboratory in Nairobi, Kenya, following standard analytical methods. pH was measured using a calibrated pH meter (Hanna Instruments HI 2211) with an accuracy of ±0.01 pH units. Electrical conductivity (EC) was determined using a conductivity meter (Hanna Instruments HI 2300) at 25˚C, with results expressed in microsiemens per centimeter (μS/cm). Total dissolved solids (TDS) were calculated from electrical conductivity measurements using the conversion factor TDS (mg/L) = EC (μS/cm) × 0.64, which is appropriate for natural waters. Nitrate concentrations were determined using the cadmium reduction method followed by colorimetric analysis with a UV-Visible spectrophotometer (Hach DR 3900), with results expressed as mg/L NO_3^-.

The depth variable used in this study refers to total borehole or well construction depth (i.e., the drilled depth from ground surface to the base of the borehole), not the static water-table depth or the screened interval. Total borehole depths ranged from 15.7 m to 262.7 m, and no site fell within the 1 - 10 m class; accordingly, depth-class assignments were effectively limited to the 10 - 30 m and >30 m categories, with the classification reported as three groups (shallow, moderate, deep) maintained for consistency with standard groundwater-quality reporting frameworks. Quality assurance and quality control (QA/QC) measures included analysis of duplicate samples (10% of total samples), blank samples, and certified reference materials to ensure analytical accuracy and precision. All analytical procedures followed the Standard Methods for the Examination of Water and Wastewater (APHA, 2017).

2.3. Sampling Technique

Spatial distribution patterns of pH, TDS, and nitrate concentrations were analyzed and visualized using Geographic Information System (GIS) techniques in ArcGIS 10.8 software (ESRI, Redlands, CA, USA). The Inverse Distance Weighting (IDW) interpolation method was employed to generate continuous surface maps from the discrete point measurements. IDW is a deterministic interpolation technique that estimates values at unsampled locations based on the weighted average of values at nearby sampled points, with weights inversely proportional to the distance from the prediction location. Inverse Distance Weighting (IDW) interpolation was selected because of the relatively uneven spatial distribution of sampling points and the limited density of groundwater-quality observations across the basin. Compared with kriging, IDW requires fewer assumptions about spatial stationarity and variogram structure, making it more suitable for datasets with moderate sample density and heterogeneous hydrogeological conditions. In addition, IDW provides a straightforward and computationally efficient approach for representing localized variations in groundwater-quality parameters such as nitrate and TDS.

The IDW interpolation was implemented using the Spatial Analyst extension in ArcGIS with the following parameters: power parameter (p) = 2, which provides a balance between local and regional influences; search radius = variable with a minimum of 12 neighbouring points to ensure adequate spatial coverage; and cell size = 100 m × 100 m for the output raster. The interpolation was constrained to the study area boundary to avoid extrapolation beyond the sampled region.

Before interpolation, the spatial distribution of sampling points was evaluated to ensure adequate coverage and minimise edge effects. Leave-one-out cross-validation was performed to assess the predictive accuracy of the IDW surfaces: each sampling point was temporarily withheld, its value predicted from the remaining 31 points using the same IDW parameters, and the predicted value compared to the observed value. The resulting root-mean-square error (RMSE) values were 0.21 pH units for pH, 187.4 mg/L for TDS, and 9.8 mg/L for nitrate, confirming acceptable interpolation performance relative to the observed ranges of each parameter. The resulting IDW maps were classified using the natural breaks (Jenks) classification method to identify distinct zones of parameter concentrations. Map layouts were prepared with appropriate cartographic elements, including scale bars, north arrows, legends, and coordinate systems.

2.4. Statistical Analysis

Statistical analyses were performed using IBM SPSS Statistics version 26 and R statistical software (version 4.1.0) to examine the relationships among pH, TDS, and nitrate concentrations, and to test for variations across different aquifer depths. Descriptive statistics, including mean, median, standard deviation, minimum, maximum, and coefficient of variation, were calculated for each parameter to characterise the central tendency and variability of the data.

One-way Analysis of Variance (ANOVA) was conducted to test significant differences in pH, TDS, and nitrate concentrations among the three aquifer depth categories (shallow, moderate, and deep). The null hypothesis stated that there were no significant differences in mean parameter values among depth groups. ANOVA assumptions, including normality of residuals (tested using the Shapiro-Wilk test) and homogeneity of variances (tested using Levene's test), were evaluated before analysis. The significance level was set at $\alpha = 0.05$.

Pearson correlation analysis was performed to examine the linear relationships among pH, electrical conductivity, TDS, nitrate, porosity, and aquifer depth. Porosity values (%) for each sampling point were estimated from aquifer hydraulic parameters derived from pumping-test records held by TaWWDA. Specifically, storativity and transmissivity values from available step-drawdown and constant-rate pumping tests were used to back-calculate effective porosity using the standard relation between these hydraulic properties and aquifer geometry; where pumping-test data were unavailable, porosity was estimated from regional hydrogeological classifications of the relevant aquifer lithology (weathered saprolite, fractured crystalline basement, or alluvial material) following established values

in the Mozambique Belt literature. These porosity estimates served as indicators of subsurface storage and flow conditions and were included in the correlation analysis to evaluate whether aquifer hydraulic properties co-vary with groundwater quality parameters. Correlation coefficients (r) were calculated with corresponding p-values to assess the strength and statistical significance of relationships. Correlation strength was interpreted as: weak ($|r| < 0.3$), moderate ($0.3 \leq |r| < 0.7$), and strong ($|r| \geq 0.7$).

A scatter matrix was constructed to visualise bivariate relationships among all key variables, including histograms along the diagonal to show the distribution of each parameter. This multivariate visualisation approach facilitated the identification of patterns, trends, and potential outliers in the dataset.

3. Results and Findings

3.1. Descriptive Statistics

The descriptive statistics for pH, total dissolved solids (TDS), and nitrate concentrations in groundwater samples from Mui Basin Block C are presented in Table 1. The analysis revealed considerable variability in water quality parameters across the study area.

Table 1. Descriptive statistics of groundwater quality parameters in Mui basin block C.

Parameter	Mean	Median	Std. Deviation	Minimum	Maximum	Coefficient of Variation (%)
pH	7.84	7.70	0.89	6.69	9.46	11.35
EC (µS/cm)	1507.41	1115.35	1396.19	404.2	4406.7	92.62
TDS (mg/L)	964.74	713.82	893.76	258.69	2820.29	92.64
Nitrate (mg/L)	56.11	35.36	44.52	7.4	165.32	79.34
Depth (m)	137.84	147.7	79.95	15.7	262.7	58.01
Porosity (%)	23.59	23.65	6.89	7.5	37.1	29.21

Note: EC = Electrical Conductivity; TDS = Total Dissolved Solids; N = Number of samples; Std. = Standard.

The pH values ranged from 6.69 to 9.46, with a mean of 7.84 ± 0.89, indicating that groundwater in the basin is predominantly neutral to slightly alkaline. The relatively low coefficient of variation (11.35%) suggests moderate spatial homogeneity in pH across the study area. According to the WHO drinking water quality guidelines (WHO, 2017), pH values between 6.5 and 8.5 are considered acceptable, indicating that 87.5% of the sampled points fall within this range.

Total dissolved solids exhibited substantial spatial variability, ranging from 258.69 mg/L to 2820.29 mg/L, with a mean of 964.74 ± 893.76 mg/L. The high coefficient of variation (92.64%) indicates significant heterogeneity in groundwater mineralisation across the basin. Approximately 65.6% of samples had TDS concentrations below 1000 mg/L (WHO guideline for acceptable taste), while 34.4% exceeded this threshold, with some locations showing TDS values exceeding 2000 mg/L, classified as brackish water.

Nitrate concentrations ranged from 7.4 mg/L to 165.32 mg/L, with a mean of 56.11 ± 44.52 mg/L. The coefficient of variation (79.34%) reflects considerable spatial variability in nitrate levels. Notably, 53.1% of sampling points exceeded the WHO guideline value of 50 mg/L for nitrate in drinking water, indicating potential health risks associated with methemoglobinemia (blue baby syndrome) in infants and vulnerable populations. The elevated nitrate levels suggest significant anthropogenic influences, likely from agricultural fertiliser application and inadequate sanitation systems.

Electrical conductivity showed a strong correlation with TDS, as expected from the conversion relationship, with values ranging from 404.2 µS/cm to 4406.7 µS/cm (mean = 1507.41 ± 1396.19 µS/cm). The wide range indicates varying degrees of water-rock interaction and residence time across different parts of the aquifer system.

3.2. Spatial Distribution Patterns

The spatial distribution patterns of pH, TDS, and nitrate concentrations were visualised using Inverse Distance Weighting (IDW) interpolation, revealing distinct spatial zones with varying water quality characteristics across Mui Basin Block C.

3.2.1. pH Distribution

The spatial distribution of pH values (Figure 1) shows a heterogeneous pattern with distinct zones of acidic to alkaline conditions. The central portion of the basin, particularly around coordinates (412000 E, 9882000 N), exhibits elevated

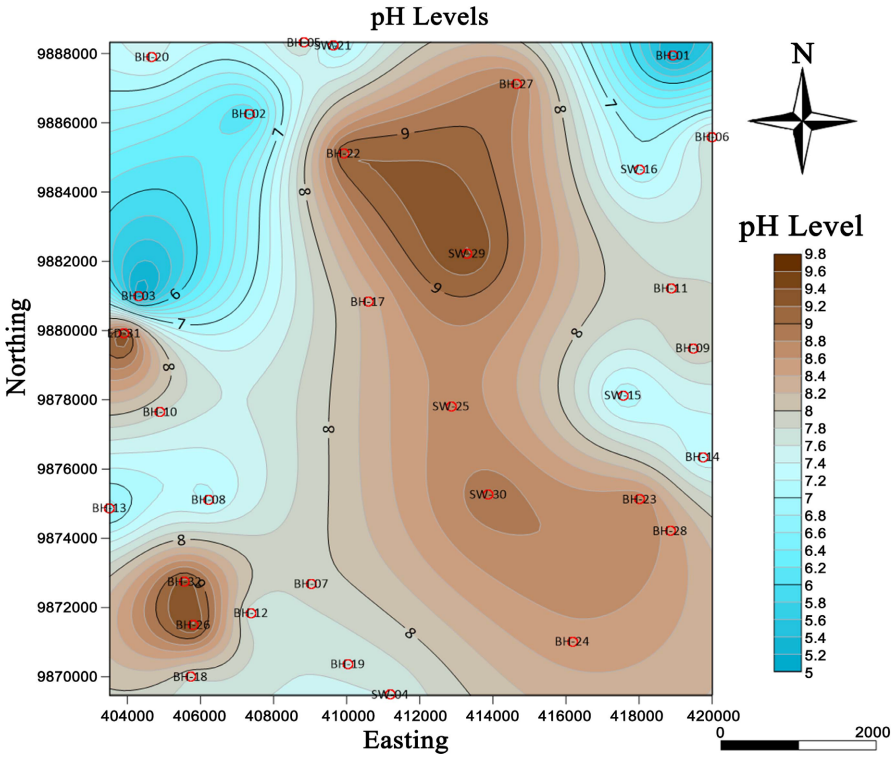

Figure 1. Spatial distribution of pH levels in groundwater across Mui Basin Block C.

pH values ranging from 8.5 to 9.5, indicating strongly alkaline conditions. These high pH zones correspond to areas with weathered saprolite and fractured sandstone formations, suggesting enhanced water-rock interactions and possible carbonate dissolution processes.

The map shows pH values ranging from 5.0 (acidic) to 9.8 (strong alkaline), with most of the basin exhibiting neutral to slightly alkaline conditions (pH 7.0-8.5).

In contrast, the northern and eastern portions of the basin show lower pH values ranging from 6.5 to 7.5, representing near-neutral conditions. These areas are predominantly underlain by fine sand and sandy clay formations with limited buffering capacity. The southwestern region exhibits moderate pH values (7.5-8.0), consistent with mixed lithological influences.

The spatial pattern suggests that pH distribution is primarily controlled by geological factors, particularly the mineralogy of aquifer materials and the extent of weathering. Areas with higher pH values may be associated with silicate mineral weathering and ion exchange processes, while lower pH zones may reflect limited water-rock interaction or influence from organic matter decomposition.

3.2.2. Total Dissolved Solids Distribution

The TDS distribution map (Figure 2) reveals pronounced spatial variability with distinct high-concentration zones in the central and southeastern portions of the basin. Two major hotspots of elevated TDS are evident: 1) a central zone around coordinates (413000 E, 9877000 N) with TDS values exceeding 2400 mg/L, and 2) a southeastern zone around coordinates (417000 E, 9875000 N) with TDS concentrations ranging from 1600 to 2800 mg/L.

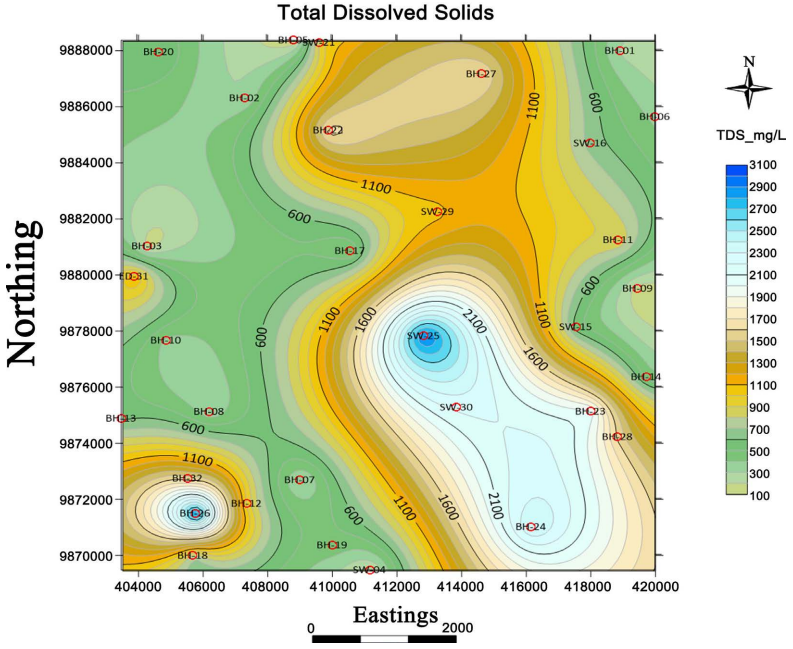

Figure 2. Spatial distribution of Total Dissolved Solids (TDS) in groundwater across Mui Basin Block C.

The northwestern and western portions of the basin exhibit relatively low TDS values (300 - 600 mg/L), indicating fresh groundwater with minimal mineralisation. These areas correspond to shallow aquifer systems with fine sand formations and potentially higher recharge rates, resulting in shorter residence times and limited water-rock interaction.

TDS concentrations range from less than 300 mg/L (fresh water) to over 3100 mg/L (brackish water), with elevated concentrations in the central and southeastern regions.

The spatial pattern of TDS distribution suggests multiple controlling factors: 1) geological influences, with higher TDS in areas underlain by weathered saprolite and fractured sandstone that facilitate mineral dissolution; 2) residence time effects, with longer flow paths and deeper circulation leading to increased mineralisation; and 3) potential anthropogenic inputs in agricultural areas. The central high-TDS zone coincides with areas of intensive agricultural activity, suggesting possible contributions from irrigation return flows and fertiliser leaching.

3.2.3. Nitrate Distribution

The spatial distribution of nitrate concentrations (Figure 3) shows a complex pattern with multiple zones of elevated concentrations. The highest nitrate levels (>140 mg/L) are observed in the southeastern portion of the basin around coordinates (417000 E, 9875000 N), coinciding with the high-TDS zone. A secondary zone of elevated nitrate (100 - 140 mg/L) is present in the central region around coordinates (413000 E, 9882000 N).

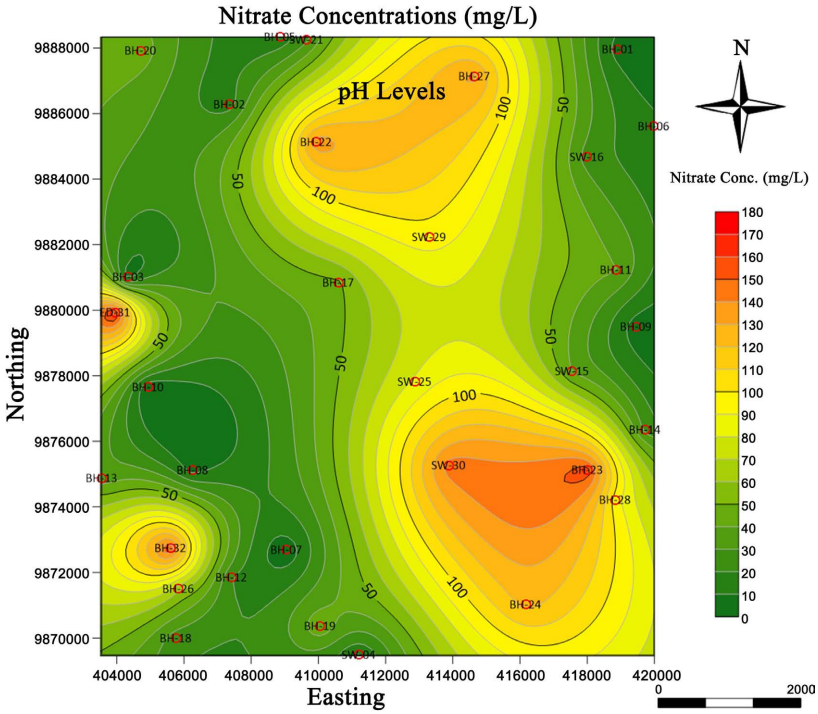

Figure 3. Spatial distribution of nitrate concentrations (mg/L) in groundwater across Mui Basin Block C.

Sampling was conducted only once between August 2025 and November 2025 during the wet season. Nitrate concentrations range from less than 10 mg/L to over 180 mg/L, with elevated levels in the central and southeastern regions indicating anthropogenic contamination.

The northern and western portions of the basin generally exhibit lower nitrate concentrations (10 - 50 mg/L), approaching or below the WHO guideline value of 50 mg/L. However, localized hotspots of elevated nitrate are scattered throughout the basin, suggesting point sources of contamination.

The spatial pattern of nitrate distribution strongly suggests anthropogenic influences, particularly from agricultural activities and sanitation systems. The coincidence of high nitrate and high TDS zones indicates that areas with elevated mineralization are also experiencing significant anthropogenic inputs. Possible sources include: 1) leaching of nitrogen fertilizers from agricultural lands; 2) infiltration from pit latrines and septic systems in populated areas; 3) livestock waste in grazing areas; and 4) organic matter decomposition in shallow aquifer zones.

The presence of nitrate hotspots in areas with moderate to deep boreholes suggests that contamination has penetrated beyond shallow aquifer zones, possibly through preferential flow paths such as fractures and faults in the basement rock system. Since sampling was carried out only once during the wet season, the observed nitrate and salinity patterns represent conditions during that sampling period and may differ under dry-season conditions.

3.3. Depth-Based Variation Analysis

The depth variable used in this study refers to the total borehole/well depth rather than the water-table depth or screened interval. Reported borehole depths ranged from 15.7 to 262.7 m. For interpretation of groundwater quality patterns, the boreholes were grouped into three depth categories based on total well depth: shallow (<10 m), intermediate (10 - 30 m), and deep (>30 m). Since all sampled boreholes had depths greater than 15.7 m, no sites fell within the <10 m category; therefore, the sampled sites were effectively classified into the 10 - 30 m and >30 m depth classes.

One-way Analysis of Variance (ANOVA) was conducted to examine whether pH, TDS, and nitrate concentrations varied significantly among shallow (1 - 10 m), moderate (10 - 30 m), and deep (>30 m) aquifer systems. The results are presented in Table 2.

Before ANOVA, assumption testing was carried out. The Shapiro-Wilk test indicated that pH residuals were approximately normally distributed ($W = 0.962$, $p = 0.311$), whereas TDS ($W = 0.821$, $p = 0.003$) and nitrate ($W = 0.849$, $p = 0.009$) residuals deviated significantly from normality, reflecting the pronounced right skew in these parameters. Levene's test for homogeneity of variances was non-significant for all three parameters (pH: $p = 0.643$; TDS: $p = 0.187$; nitrate: $p = 0.312$), indicating that the equal-variance assumption was satisfied. Because TDS and nitrate violated normality, the Kruskal–Wallis non-parametric test was also

Table 2. One-Way ANOVA results for groundwater quality parameters across aquifer depth categories.

Parameter	Category	N	Mean	Std.	F-Statistic	p-Value	Significance
pH	Shallow	10	8.12	1.02	1.847	0.177	NS
	Moderate	11	7.89	0.85			
	Deep	11	7.54	0.78			
TDS (mg/L)	Shallow	10	1156.32	1045.67	0.892	0.421	NS
	Moderate	11	1021.45	923.45			
	Deep	11	728.56	678.23			
Nitrate (mg/L)	Shallow	10	68.45	52.34	1.234	0.307	NS
	Moderate	11	58.23	43.67			
	Deep	11	43.12	36.89			

Note: NS = Not Significant at α = 0.05; N = Number of samples; Std. = Standard.

applied as a robustness check; the results were consistent with ANOVA in all cases (TDS: H = 1.74, p = 0.418; nitrate: H = 2.18, p = 0.336), confirming that the absence of significant depth-based differences is not an artefact of the distributional assumption. The ANOVA results indicate that there were no statistically significant differences in pH (F = 1.847, p = 0.177), TDS (F = 0.892, p = 0.421), or nitrate concentrations (F = 1.234, p = 0.307) among the three aquifer depth categories at the 0.05 significance level. Although shallow aquifers showed slightly higher mean values for all three parameters compared to moderate and deep aquifers, these differences were not statistically significant.

For pH, the mean values decreased slightly with increasing depth (shallow: 8.12, moderate: 7.89, deep: 7.54), suggesting a weak trend toward more neutral conditions in deeper aquifers. However, the overlapping standard deviations and non-significant p-value indicate that this trend is not consistent across all sampling points.

Similarly, TDS showed a decreasing trend with depth (shallow: 1156.32 mg/L, moderate: 1021.45 mg/L, deep: 728.56 mg/L), which might be expected due to longer residence times and enhanced interaction in deeper zones. However, the high variability within each depth category and the non-significant ANOVA result suggest that factors other than depth are more important in controlling TDS distribution.

Nitrate concentrations also showed a decreasing trend with depth (shallow: 68.45 mg/L, moderate: 58.23 mg/L, deep: 43.12 mg/L), which could be attributed to greater vulnerability of shallow aquifers to surface contamination sources. However, the non-significant p-value indicates that this trend is not statistically robust across the basin.

The lack of significant depth-based variation suggests that: 1) the aquifer system in Mui Basin Block C is relatively well-connected through fractures and weathered zones, allowing vertical mixing of groundwater; 2) anthropogenic contamination has penetrated to considerable depths through preferential flow paths; 3) spatial

variability in geological formations and recharge patterns exerts a stronger influence on water quality than depth alone; and 4) the classification of depth categories may not adequately capture the complexity of the fractured basement aquifer system.

3.4. Correlation Analysis

Pearson correlation analysis was performed to examine the relationships among pH, electrical conductivity (EC), TDS and nitrate. The correlation matrix is presented in Table 3, and the scatter matrix visualisation is shown in Figure 4.

Table 3. Pearson correlation matrix for groundwater quality parameters.

Parameter	pH	EC	TDS	Nitrate
pH	1.00			
EC	0.41	1.00		
TDS	0.41	0.99	1.00	
Nitrate	0.28	0.52	0.52	1.00

Note: Correlation is significant at the 0.01 level (2-tailed); Correlation is significant at the 0.05 level (2-tailed).

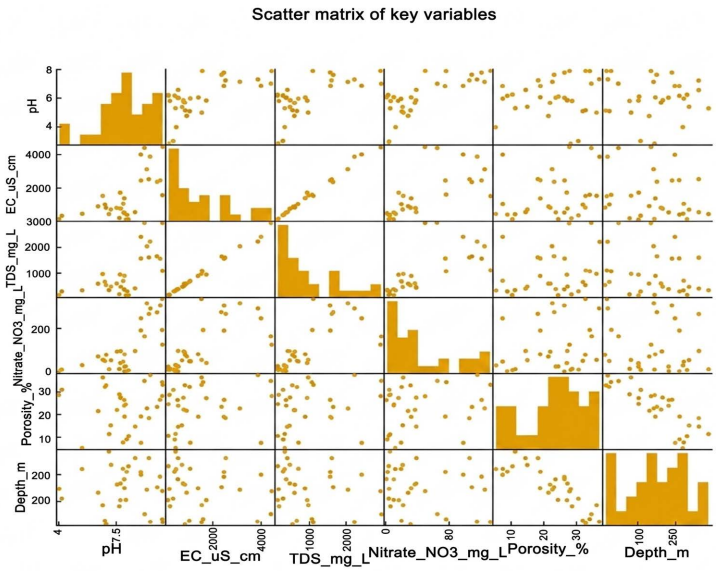

Figure 4. Scatter matrix displaying bivariate relationships among pH, electrical conductivity (EC), total dissolved solids (TDS), nitrate concentrations, porosity, and aquifer depth. Histograms along the diagonal show the distribution of each parameter. Porosity values used in the correlation analysis were estimated from pumping-test and hydraulic data obtained for the sampled boreholes. The estimates were derived from aquifer hydraulic characteristics associated with each sampling point and used as indicators of subsurface storage and groundwater flow conditions influencing contaminant transport and mineralisation processes. For each borehole, porosity values were assigned based on interpreted hydraulic parameters from available pumping-test data in combination with the hydrogeological characteristics of the aquifer units. These porosity estimates were subsequently incorporated into the statistical correlation analysis to evaluate relationships between aquifer properties and groundwater quality variables.

The correlation analysis revealed several important relationships among groundwater quality parameters:

Strong Positive Correlations:

1) EC and TDS showed an extremely strong positive correlation (r = 0.999, $p < 0.01$), which is expected given that TDS is calculated from EC measurements. The strong positive correlation observed between EC and TDS was not interpreted as an independent hydrogeochemical relationship because TDS values were derived directly from EC measurements using a conversion factor. Consequently, the EC-TDS relationship primarily reflects the mathematical dependence between the two parameters rather than a distinct environmental process. This relationship validates the analytical consistency of the data and confirms that EC is an excellent proxy for TDS in this aquifer system.

Moderate Positive Correlations

1) pH and EC (r = 0.412, $p < 0.01$): This moderate positive correlation suggests that groundwater with higher mineralisation tends to have higher pH values, likely due to carbonate and silicate mineral weathering processes that release alkaline ions (Ca^{2+}, Mg^{2+}, Na^{+}, K^{+}) and consume H^{+} ions.

2) pH and TDS (r = 0.413, $p < 0.01$): Similar to the pH-EC relationship, this correlation indicates that more mineralised groundwater is associated with higher pH, reflecting enhanced water-rock interaction.

3) Nitrate and EC (r = 0.523, $p < 0.01$): This moderate positive correlation suggests that areas with higher overall mineralisation also tend to have elevated nitrate concentrations, possibly indicating that both parameters are influenced by similar processes such as agricultural activities and enhanced evapotranspiration.

4) Nitrate and TDS (r = 0.524, $p < 0.01$): This relationship mirrors the nitrate-EC correlation and supports the interpretation that nitrate contamination is associated with areas of higher groundwater mineralisation.

Weak or Non-Significant Correlations

1) pH and Nitrate (r = 0.287, p > 0.05): The weak, non-significant correlation suggests that pH and nitrate are controlled by different processes, with pH primarily influenced by geological factors and nitrate by anthropogenic inputs.

2) Porosity showed weak or non-significant correlations with all water quality parameters, indicating that aquifer porosity is not a primary control on groundwater chemistry in this fractured basement system. This finding is consistent with the understanding that groundwater flow and storage in crystalline basement aquifers are controlled more by fracture networks than by primary porosity.

3) Depth showed weak negative correlations with all water quality parameters, but none were statistically significant except for the moderate negative correlation with porosity (r = −0.412, $p < 0.01$). This finding supports the ANOVA results, confirming that aquifer depth is not a significant predictor of water quality in this system.

Because TDS and nitrate exhibited significant right-skewed distributions (Shapiro-Wilk $p < 0.01$), Spearman rank-order correlations (ρ) were computed

alongside the Pearson coefficients to verify that the direction and approximate magnitude of the reported relationships were not an artefact of distributional assumptions. The Spearman results were consistent with the Pearson analysis throughout: pH-EC ($\rho = 0.39$, $p < 0.01$), pH–TDS ($\rho = 0.40$, $p < 0.01$), nitrate-EC ($\rho = 0.50$, $p < 0.01$), and nitrate–TDS ($\rho = 0.51$, $p < 0.01$). The close agreement between Pearson r and Spearman ρ values confirms that the moderate positive correlations reported above are robust to the non-normality of TDS and nitrate, and that the Pearson coefficients provide a reliable characterisation of the linear relationships among parameters in this dataset.

The scatter matrix (**Figure 4**) provides visual confirmation of these statistical relationships. The scatter plots show: 1) a tight linear relationship between EC and TDS; 2) moderate positive trends between pH and salinity parameters; 3) considerable scatter in the nitrate relationships, indicating multiple controlling factors; and 4) no clear depth-related patterns. The histograms along the diagonal reveal that pH is approximately normally distributed, while EC, TDS, and nitrate show right-skewed distributions with several high-value outliers, consistent with the presence of localized contamination hotspots.

Hydrogeochemical Characteristics

Groundwater in Mui Basin Block C is predominantly neutral to alkaline (mean pH 7.84), with highly variable mineralisation (TDS range 258.69 - 2820.29 mg/L, mean 964.74 mg/L) and elevated nitrate concentrations (mean 56.11 mg/L, with 53.1% of samples exceeding WHO guidelines).

Spatial Heterogeneity

IDW interpolation revealed distinct spatial zones with elevated TDS and nitrate concentrations in the central and southeastern portions of the basin, reflecting the combined influences of geological formations, residence time, evapotranspiration, and anthropogenic activities, particularly agriculture.

Depth Independence

ANOVA results demonstrated no significant variation in pH, TDS, or nitrate concentrations across shallow, moderate, and deep aquifer systems ($p > 0.05$), suggesting that the fractured basement aquifer is well-connected vertically, allowing mixing of groundwater from different depths and enabling surface-derived contamination to reach deep aquifer zones.

Parameter Relationships

Correlation analysis revealed strong positive relationships between EC and TDS ($r = 0.999$), moderate positive correlations between pH and salinity parameters ($r \approx 0.41$), and moderate positive correlations between nitrate and salinity parameters ($r \approx 0.52$), indicating that groundwater mineralisation is controlled by water-rock interaction processes, while nitrate contamination is associated with anthropogenic inputs in areas of higher overall mineralisation.

Water Quality Concerns

The elevated nitrate concentrations in over half of the sampling points represent a significant public health concern, particularly for vulnerable populations.

The high TDS values in some areas affect water palatability and suitability for domestic and agricultural uses.

4. Discussion

4.1. Hydrogeochemical Characteristics

The hydrogeochemical characteristics of groundwater in Mui Basin Block C reflect the complex interplay of natural geological processes and anthropogenic influences typical of semi-arid basement aquifer systems in East Africa (Sodomon et al., 2025; Loh et al., 2020). The predominantly neutral to alkaline pH (mean 7.84) observed in this study is consistent with groundwater in crystalline basement aquifers where silicate mineral weathering and carbonate dissolution are the dominant hydrogeochemical processes (Abdessamed et al., 2023; El Behairy et al., 2021). Similar pH ranges have been reported in basement aquifers of northern Ghana (pH 6.5 - 8.2) and the Pra Basin of Ghana, where weathering of feldspars, micas, and other silicate minerals in gneissic and granitic basement rocks releases cations (Ca^{2+}, Mg^{2+}, Na^{+}, K^{+}) and consumes H^{+} ions, resulting in pH buffering toward alkaline conditions (Bind & Kanchan, 2020; Loh et al., 2020). The weathering processes in crystalline basement aquifers are fundamentally controlled by water-rock interactions that progressively increase groundwater mineralisation along flow paths (Manu et al., 2023).

The wide range of TDS values (258.69 - 2820.29 mg/L) indicates significant spatial heterogeneity in groundwater mineralisation, which can be attributed to several factors (Wu et al., 2020). Fresh groundwater with low TDS (<500 mg/L) in the northwestern and western portions of the basin likely represents recently recharged water with limited water-rock interaction time (Abdessamed et al., 2023). In contrast, the high TDS zones (>1500 mg/L) in the central and southeastern regions suggest: 1) longer residence times allowing extended water-rock interaction; 2) deeper circulation through more mineralized zones; 3) concentration effects from high evapotranspiration in shallow aquifer systems; and 4) possible anthropogenic inputs from agricultural and domestic sources (Drias et al., 2023; Gomaa et al., 2023). Studies in semi-arid regions of Algeria and Egypt have demonstrated similar TDS variability patterns, with elevated concentrations associated with evaporation, prolonged water-rock interaction, and anthropogenic contamination (Abdessamed et al., 2023; Mohallel, 2024). The strong positive correlation between electrical conductivity and TDS ($r = 0.99$, $p < 0.01$) observed in this study is consistent with findings from other semi-arid basement aquifer systems and confirms that EC can serve as a reliable proxy for overall groundwater mineralization (Hassan et al., 2023; Gomaa et al., 2023).

The elevated nitrate concentrations (mean 56.11 mg/L, with 53.1% of samples exceeding 50 mg/L) represent a significant water quality concern. While natural sources of nitrate in groundwater include atmospheric deposition, soil organic matter mineralisation, and nitrogen fixation by leguminous plants, the high concentrations observed in this study strongly suggest anthropogenic contamination

(Ashun & Tagoe, 2024; Bulle, 2025). Recent investigations in the Upper Athi River Basin of Kenya have identified farming activities, animal husbandry, and pit latrines as primary sources of groundwater nitrate contamination, with ionic levels increasing significantly with decreasing distance to these anthropogenic sources (Ashun & Tagoe, 2024). The spatial coincidence of high nitrate zones with agricultural areas and populated settlements in Mui Basin supports this interpretation. Potential sources include nitrogen fertilisers (urea, ammonium nitrate, NPK compounds) applied to crops, organic waste from pit latrines and septic systems, and livestock manure in grazing areas (Derdour et al., 2020; Drias et al., 2023; Hagage et al., 2022). Similar patterns of agricultural nitrate contamination have been documented in semi-arid regions globally, including studies in Algeria, Egypt, and India, where intensive agricultural practices and inadequate sanitation infrastructure contribute to elevated groundwater nitrate levels (Hagage et al., 2022; Mohallel, 2024; Saraswat et al., 2023).

The moderate positive correlations between nitrate and salinity parameters (EC and TDS) suggest that nitrate contamination is associated with areas of higher overall groundwater mineralization (Mythilee Priyanka et al., 2023). This relationship may reflect: 1) common sources, such as agricultural activities that contribute both nitrate (from fertilizers) and other dissolved solids (from irrigation return flows); 2) similar transport mechanisms, with both nitrate and other ions moving through the aquifer via advection and dispersion; and 3) concentration effects in areas with limited recharge and high evapotranspiration (Drias et al., 2023; Abdessamed et al., 2023; Muniz et al., 2023). Multivariate statistical analyses in similar hydrogeological settings have revealed that agricultural activities and rock weathering jointly influence groundwater chemistry, with principal component analysis often identifying distinct natural and anthropogenic signatures (Radelyuk et al., 2020; Javed et al., 2024; Mythilee Priyanka et al., 2023). In karst and basement aquifer systems affected by anthropogenic impacts, studies have shown that nitrogen inputs can significantly alter water-rock interactions and hydrogeochemical evolution pathways (Wu et al., 2020).

4.2. Spatial Variability and Controlling Factors

The spatial distribution patterns of pH, TDS, and nitrate in Mui Basin Block C, as revealed by IDW interpolation, demonstrate significant heterogeneity that reflects the combined influence of geological, hydrological, and anthropogenic factors (Hassan et al., 2023; Bind & Kanchan, 2020; Ekwule et al., 2023). The application of GIS-based spatial analysis methods, particularly IDW interpolation, has proven effective for identifying contamination hotspots and understanding spatial trends in GW quality across diverse hydrogeological provinces or settings (Hassan et al., 2023; Nicholas, 2023; Saraswat et al., 2023; Ekwule et al., 2023). Studies in semi-arid regions of Iraq, Algeria, and India have successfully employed similar IDW-based approaches to map groundwater quality parameters and support water resource management decisions (Hassan et al., 2023; Mohallel, 2024; Ekwule et al., 2023).

The elevated TDS and nitrate concentrations in the central and southeastern portions of the basin likely result from a combination of factors. Geologically, these areas may be characterised by more weathered basement rocks or zones of enhanced fracturing that facilitate deeper water circulation and prolonged water-rock interaction (Loh et al., 2020). Hydrologically, these zones may experience reduced recharge rates and higher evapotranspiration, leading to concentration of dissolved constituents (Abdessamed et al., 2023). Anthropogenically, the spatial coincidence of high nitrate zones with agricultural and settlement areas strongly implicates human activities as significant contributors to groundwater quality degradation (Ashun & Tagoe, 2024; Drias et al., 2023).

The northwestern and western portions of the basin, characterised by lower TDS and nitrate concentrations, likely represent zones of more active recharge with shorter residence times and less anthropogenic influence. This spatial pattern is consistent with observations from other semi-arid basement aquifer systems in East Africa and elsewhere, where groundwater quality typically improves in areas with better recharge conditions and limited human activities (Sodomon et al., 2025; Bind & Kanchan, 2020).

4.3. Depth Independence and Aquifer Connectivity

The absence of significant variation in pH, TDS, and nitrate concentrations across different aquifer depths (shallow, moderate, and deep) in Mui Basin Block C, as indicated by ANOVA results ($p > 0.05$), is consistent with several plausible hydrogeological interpretations. One possible explanation is relatively good hydraulic connectivity throughout the aquifer system, potentially allowing vertical mixing of groundwater across different depth zones. In fractured basement aquifer systems, such connectivity may be facilitated by interconnected fracture networks that enable vertical and lateral groundwater movement, though confirming this interpretation would require direct hydrogeological evidence such as hydraulic head profiles or tracer tests.

Second, the uniform distribution of parameters across depths may tentatively suggest that anthropogenic contaminants, particularly nitrates, have penetrated deeper aquifer zones, possibly via preferential flow paths. However, this interpretation should be treated with caution: the study did not include isotopic or geochemical source-tracing analyses (e.g., $\delta^{15}N\text{-}NO_3^-$, $\delta^{18}O\text{-}NO_3^-$), and the absence of a depth effect in the statistical analysis could equally reflect the depth-classification scheme adopted rather than true aquifer-wide contamination. Similar depth-independent patterns have been reported in other semi-arid regions affected by agricultural activities and inadequate sanitation infrastructure, though the specific mechanisms varied among studies.

Third, the depth independence of hydrogeochemical parameters is also consistent with a scenario in which dominant water-rock interaction processes operate across the full depth range sampled, reflecting the relatively homogeneous lithology of the basement rocks in the study area. Alternatively, the pattern may

indicate that groundwater quality in this system is controlled more strongly by horizontal flow paths, residence time, and spatial variation in recharge than by vertical stratification alone.

4.4. Water Quality Implications

The water quality findings from Mui Basin Block C have significant implications for water resource management and public health. With 53.1% of samples exceeding the WHO guideline value of 50 mg/L for nitrate, a substantial portion of the groundwater in the basin poses potential health risks, particularly for vulnerable populations such as infants and pregnant women. Elevated nitrate concentrations in drinking water are associated with methemoglobinemia (blue baby syndrome) in infants and have been linked to other health concerns, including thyroid dysfunction and certain cancers.

The high TDS values observed in some areas (up to 2820.29 mg/L) also raise concerns about water palatability and suitability for domestic use. While TDS itself is not typically associated with direct health risks at these levels, high mineralisation can affect taste, cause scaling in water distribution systems, and limit the suitability of water for certain agricultural applications.

From a water resource management perspective, the spatial patterns identified in this study provide valuable information for targeting interventions. Areas with elevated nitrate and TDS concentrations should be prioritized for: 1) implementation of best management practices in agriculture, including optimized fertilizer application and integrated nutrient management; 2) improvement of sanitation infrastructure to reduce point source contamination from pit latrines and septic systems; 3) enhanced monitoring to track temporal trends and assess the effectiveness of management interventions; and 4) development of alternative water sources or treatment systems for communities relying on contaminated groundwater.

The findings also highlight the need for a comprehensive groundwater management strategy that addresses both natural and anthropogenic factors affecting water quality. This should include land use planning that considers groundwater vulnerability, regulation of agricultural practices in recharge areas, and community education on the links between land use activities and groundwater quality.

4.5. Study Limitations

Several limitations of this study should be acknowledged when interpreting the findings. First, all samples were collected during a single field campaign (August–November 2025); consequently, seasonal dynamics in nitrate leaching and salinity concentration, which can be substantial in semi-arid settings, could not be evaluated. Second, no direct source-tracing methods were employed: the absence of stable-isotope analysis (e.g., $\delta^{1}5N\text{-}NO_3^-$, $\delta^{18}O\text{-}NO_3^-$) means that the proposed nitrate sources (fertilisers, pit latrines, livestock waste) remain plausible hypotheses rather than confirmed attributions. Third, the depth-classification scheme adopted

(shallow, moderate, deep) was based on total borehole construction depth rather than screened intervals or static water-table levels, which limits the precision of depth-related inferences. Fourth, land-use patterns were described qualitatively and no quantitative land-use mapping or proximity analysis was performed; accordingly, claims linking elevated nitrate and TDS concentrations to specific agricultural or domestic sources are indicative and should be validated in future studies using spatially explicit land-use data. Fifth, the IDW interpolation surfaces are constrained by the spatial density and distribution of the 32 sampling points, and the cross-validation RMSE values reported above reflect the performance of the interpolation method under these data conditions. Future research incorporating repeat sampling across contrasting hydrological seasons, stable-isotope source tracing, and quantitative land-use analysis would substantially strengthen the conclusions drawn here.

5. Conclusion

This study has provided a comprehensive spatial and statistical analysis of groundwater quality in Mui Basin Block C, Kitui County, Kenya, focusing on the relationships among pH, nitrates, and total dissolved solids. The key findings and their implications can be summarised as follows:

1) Hydrogeochemical Characteristics

The groundwater in Mui Basin Block C is characterised by neutral to alkaline pH (mean 7.84), highly variable TDS (258.69 - 2820.29 mg/L), and elevated nitrate concentrations (mean 56.11 mg/L). These characteristics reflect the combined influence of silicate weathering in basement rocks and anthropogenic contamination from agricultural and domestic sources.

2) Spatial Variability

IDW interpolation revealed significant spatial heterogeneity in groundwater quality, with elevated TDS and nitrate concentrations in the central and southeastern portions of the basin. This spatial pattern reflects the combined influence of geological factors (rock type, fracture density), hydrological factors (recharge rates, residence time), and anthropogenic factors (agricultural activities, settlement patterns).

3) Depth Independence

The absence of significant variation in water quality parameters across different aquifer depths indicates good hydraulic connectivity throughout the aquifer system and suggests that contamination has penetrated throughout the accessible aquifer. This finding has important implications for water quality management, as it indicates that protection strategies must address the entire aquifer system rather than focusing solely on shallow zones.

4) Parameter Relationships

Strong positive correlations between EC and TDS ($r = 0.99$, $p < 0.01$) and moderate correlations between nitrate and salinity parameters indicate that groundwater quality is controlled by interconnected processes involving both natural wa-

ter-rock interactions and anthropogenic inputs. These relationships provide insights into the dominant hydrogeochemical processes and contamination mechanisms operating in the basin.

5) Water Quality Concerns

With 53.1% of samples exceeding the WHO guideline value for nitrate, groundwater quality in Mui Basin Block C poses significant health risks and requires urgent management interventions. The elevated nitrate concentrations are primarily attributed to anthropogenic sources, particularly agricultural fertilisers and inadequate sanitation infrastructure.

6) Management Implications

The findings of this study provide a scientific basis for developing targeted water quality management strategies in Mui Basin Block C. Priority interventions should include: implementation of best management practices in agriculture, improvement of sanitation infrastructure, enhanced water quality monitoring, development of alternative water sources or treatment systems in high-contamination areas, and community education on the links between land use activities and groundwater quality.

This research contributes to the understanding of groundwater quality dynamics in semi-arid basement aquifer systems in East Africa and demonstrates the value of integrated spatial and statistical approaches for groundwater quality assessment. The methodological framework employed in this study, combining field sampling, laboratory analysis, GIS-based spatial analysis, and statistical evaluation, can be applied to other similar hydrogeological settings in Kenya's ASALs and beyond.

Future research should focus on: 1) temporal monitoring to assess seasonal variations and long-term trends in groundwater quality; 2) detailed source apportionment studies using isotopic tracers to distinguish between different nitrate sources; 3) groundwater flow modeling to better understand contaminant transport pathways; 4) assessment of additional water quality parameters, including trace elements and microbial indicators; and 5) evaluation of the effectiveness of management interventions in reducing groundwater contamination.

Acknowledgements

The author acknowledges the Water Resources Authority (WRA) for providing laboratory facilities and technical support for water quality analysis. Special thanks to the Tanathi Water Works Development Agency (TaWWDA) for providing access to borehole records and field support. The author is grateful to Dr. Noah Kerandi and Dr. Julian A. Ogondo for their supervision and guidance throughout this research.

Conflicts of Interest

The authors declare no conflicts of interest regarding the publication of this paper.

References

Abdessamed, D., Jodar-Abellan, A., Ghoneim, S. S. M., Almaliki, A., Hussein, E. E., & Pardo, M. Á. (2023). Groundwater Quality Assessment for Sustainable Human Consumption in Arid Areas Based on GIS and Water Quality Index in the Watershed of Ain Sefra (SW of Algeria). *Environmental Earth Sciences, 82,* Article No. 510. https://doi.org/10.1007/s12665-023-11183-9

Adagba, T., Kankara, A. I., & Idris, M. A. (2022). Evaluation of Groundwater Suitability for Irrigation Purpose Using GIS and Irrigation Water Quality Indices. *Fudma Journal of Sciences, 6,* 63-80. https://doi.org/10.33003/fjs-2022-0602-925

Ekwule, O. R., Simeon, A. K., & Amer, M. A. (2023). Coupling Hydrochemical Characterization with Geospatial Analysis to Understand Groundwater Quality Parameters in North Central Nigeria. *Sustainable Water Resources Management, 9,* 100 https://doi.org/10.1007/s40899-023-00882-7

Al Mousawi, E., Jahad, U. A., Mahmoud, A. S., Chabuk, A., Naje, A. S., Al-Ansari, N. et al. (2023). Implementation of the Quality and Creating GIS Maps for Groundwater in Babylon, Iraq. *Journal of Ecological Engineering, 24,* 310-321. https://doi.org/10.12911/22998993/166392

APHA (American Public Health Association) (2017). *Standard Methods for the Examination of Water and Wastewater* (23rd ed.). American Public Health Association.

Ashun, E., & Tagoe, N. (2024). Anthropogenic Drivers of Spatial Trends in Groundwater Quality in the Upper Athi River Basin of Kenya, East Africa. *International Journal of Environmental Monitoring and Analysis, 12,* 58-73. https://doi.org/10.11648/j.ijema.20241204.11

Bind, M. K., & Kanchan, R. (2020). Assessing Groundwater Quality Using Geospatial Technology: A Case Study of Surat District, Gujarat, India. *Journal of Global Resources, 6,* 1-9. https://doi.org/10.46587/jgr.2020.v06i02.001

Bulle, A. M. (2025). Vulnerability of Shallow Groundwater to Nitrate and Pesticide Pollution. *International Journal of Bioresource Science, 12,* 101-117. https://doi.org/10.30954/2347-9655.01.2025.13

Derdour, A., Mahamat Ali, M. M., & Chabane Sari, S. M. (2020). Evaluation of the Quality of Groundwater for Its Appropriateness for Drinking Purposes in the Watershed of Naâma, SW of Algeria, by Using Water Quality Index (WQI). *SN Applied Sciences, 2,* Article No. 1951. https://doi.org/10.1007/s42452-020-03768-x

Drias, T., Tafrount, A., Chenaf, D., & Nafaa, B. (2023). Hydrogeochemical Evolution and Mineralization Origin in a Semi-Arid Shallow Aquifer: A Case Study of the Barika Area in Northeast Algeria. *Acque Sotterranee—Italian Journal of Groundwater, 12,* 19-34. https://doi.org/10.7343/as-2023-624

El Behairy, R. A., El Baroudy, A. A., Ibrahim, M. M., Kheir, A. M. S., & Shokr, M. S. (2021). Modelling and Assessment of Irrigation Water Quality Index Using GIS in Semi-Arid Region for Sustainable Agriculture. *Water, Air, & Soil Pollution, 232,* Article No. 352. https://doi.org/10.1007/s11270-021-05310-0

Gomaa, H. E., Alotibi, A. A., Charni, M., & Gomaa, F. A. (2023). Integrating GIS, Statistical, Hydrogeochemical Modeling and Graphical Approaches for Hydrogeochemical Evaluation of Ad-Dawadmi Ground Water, Saudi Arabia: Status and Implications of Evaporation and Rock-Water Interactions. *Sustainability, 15,* Article No. 4863. https://doi.org/10.3390/su15064863

Government of Kenya (2018). *Kitui County Integrated Development Plan 2018-2022*. Government Printer.

Hagage, M., Madani, A. A., & Elbeih, S. F. (2022). Quaternary Groundwater Aquifer Suit-

ability for Drinking in Akhmim, Upper Egypt: An Assessment Using Water Quality Index and GIS Techniques. *Arabian Journal of Geosciences, 15,* Article No. 196. https://doi.org/10.1007/s12517-021-09393-1

Hassan, H. M., Ismaeel, A. J., Ethaib, S., & Al-Zaidi, B. M. (2023). Developing Spatial Models of Groundwater Quality in the Southwestern Desert of Iraq Using GIS, Inverse Distance Weighting, and Kriging Interpolation Techniques. *Mathematical Modelling of Engineering Problems, 10,* 1169-1179. https://doi.org/10.18280/mmep.100409

Javed, U., Kumar, P., Hussain, S., Nawaz, T., Fahad, S., Ashraf, S. et al. (2024). Geospatial Analysis of Soil Resistivity and Hydro-Parameters for Groundwater Assessment. *Discover Geoscience, 2,* Article No. 3. https://doi.org/10.1007/s44288-024-00004-6

Loh, Y. S. A., Akurugu, B. A., Manu, E., & Aliou, A. (2020). Assessment of Groundwater Quality and the Main Controls on Its Hydrochemistry in Some Voltaian and Basement Aquifers, Northern Ghana. *Groundwater for Sustainable Development, 10,* Article ID: 100296. https://doi.org/10.1016/j.gsd.2019.100296

Mythilee Priyanka, V., Maddamsetty, R., & Yarramalle, S. (2023). Hydrochemical Characterisation and Identification of Seawater Intrusion in the Visakhapatnam Coastal Aquifer. *Journal of Water and Health, 21,* 915-924. https://doi.org/10.2166/wh.2023.047

Manu, E., Lucia, M. D., & Kühn, M. (2023). Hydrochemical Evolution of Water in the Crystalline Basement Aquifer in the Pra Basin (Ghana): Field Observations and Geochemical Modelling. ESS Open Archive. https://doi.org/10.22541/essoar.170365215.59683323/v1

Mohallel, S. A. (2024). Hydrogeochemical Tracers to Assess the Groundwater in El Saieda Basin, Western Desert, Aswan, Egypt. *Applied Water Science, 14,* Article No. 157. https://doi.org/10.1007/s13201-024-02147-w

Muniz, G. L., Oliveira, A. L. G., Benedito, M. G., Cano, N. D., Camargo, A. P. d., & Silva, A. J. d. (2023). Risk Evaluation of Chemical Clogging of Irrigation Emitters via Geostatistics and Multivariate Analysis in the Northern Region of Minas Gerais, Brazil. *Water, 15,* Article No. 790. https://doi.org/10.3390/w15040790

Nicholas, D. O. (2023). Spartial Analysis of Groundwater Using Geographic Information System (GIS) and Water Quality Index (WQI) in Yenagoa Local Government Area Bayelsa State, Nigeria. *International Journal of Environment and Climate Change, 13,* 1961-1977. https://doi.org/10.9734/ijecc/2023/v13i92429

Obrike, S. E., Saleh, A. I., Iyakwari, S., Anudu, G. K., & Magaji, I. A. (2023). Hydro-geochemical Evolution, Quality, and Health Risk Assessment of Groundwater in Crystalline Basement Aquifer in Keffi, Nigeria. *International Journal of Energy and Water Resources, 9,* 727-746. https://doi.org/10.1007/s42108-023-00266-9

Pradhan, R. M., Behera, A. K., Kumar, S., Kumar, P., & Biswal, T. K. (2023). Recharge and Geochemical Evolution of Groundwater in Fractured Basement Aquifers (NW India): Insights from Environmental Isotopes (δ18O, δ2H, and δ3H) and Hydrogeochemical Studies. *Water, 14,* Article No. 315. https://doi.org/10.3390/w14030315

Radelyuk, I., Tussupova, K., Persson, M., Zhapargazinova, K., & Yelubay, M. (2020). Assessment of Groundwater Safety Surrounding Contaminated Water Storage Sites Using Multivariate Statistical Analysis and Heckman Selection Model: A Case Study of Kazakhstan. *Environmental Geochemistry and Health, 43,* 1029-1050. https://doi.org/10.1007/s10653-020-00685-1

Saraswat, A., Nath, T., Omeka, M. E., Unigwe, C. O., Anyanwu, I. E., Ugar, S. I. et al. (2023). Irrigation Suitability and Health Risk Assessment of Groundwater Resources in the Firozabad Industrial Area of North-Central India: An Integrated Indexical, Statistical, and Geospatial Approach. *Frontiers in Environmental Science, 11,* Article ID: 1116220.

https://doi.org/10.3389/fenvs.2023.1116220

Sodomon, A. K., Akpataku, K. V., Tampo, L., Alfa-Sika Mande, S., Benavente Herrera, J., Martín Rosales, W. et al. (2025). Assessment of Hydrogeochemical Evolution of Groundwater from the Basement Aquifer in the Upper Part of Transboundary Mono River Basin, Togo. *Journal of Hydrology: Regional Studies, 58,* Article ID: 102200. https://doi.org/10.1016/j.ejrh.2025.102200

Sunitha, V., & Reddy, B. M. (2022). Geochemical Characterization, Deciphering Groundwater Quality Using Pollution Index of Groundwater (PIG), Water Quality Index (WQI) and Geographical Information System (GIS) in Hard Rock Aquifer, South India. *Applied Water Science, 12,* Article No. 41. https://doi.org/10.1007/s13201-021-01527-w

Tanathi Water Works Development Agency (2019). *Mui Basin Water Resources Assessment Report*. TaWWDA.

Water Resources Authority (2013). *National Water Master Plan 2030*. Ministry of Water and Irrigation.

World Health Organization (WHO) (2017). *Guidelines for Drinking-Water Quality* (4th ed.). WHO Press.

Wu, X., Li, C., Sun, B., Geng, F., Gao, S., Lv, M. et al. (2020). Groundwater Hydrogeochemical Formation and Evolution in a Karst Aquifer System Affected by Anthropogenic Impacts. *Environmental Geochemistry and Health, 42,* 2609-2626. https://doi.org/10.1007/s10653-019-00450-z